

Nonlinear Superconducting Magnetoelectric Effect

Jin-Xin Hu,^{1,*} Oles Matsyshyn,¹ and Justin C. W. Song^{1,†}

¹*Division of Physics and Applied Physics, School of Physical and Mathematical Sciences, Nanyang Technological University, Singapore 637371*

A supercurrent flow can induce a nonvanishing spin magnetization in noncentrosymmetric superconductors with spin-orbit interaction. Often known as the non-dissipative magnetolectric effect, these are most commonly found at linear order in supercurrent flow. Here, we argue that a *nonlinear* superconducting magnetolectric effect (NSM) can naturally manifest in altermagnet/superconductor (ALM/SC) heterostructures: NSM manifests as a spin polarization generated as a second-order response to a driving supercurrent. Strikingly, we find NSM is the leading order magnetization response in ALM/SC heterostructures and survives even in the presence of centrosymmetry; $C_4\mathcal{T}$ symmetry in altermagnets zeroes both the equilibrium magnetization as well as out-of-plane linear magnetolectric response. This renders NSM a powerful electric and non-dissipative means of controlling magnetization in ALM/SC heterostructures, a promising platform for superconducting spintronics.

Introduction.—Unlike the normal metallic state, the intrinsically non-dissipative flow of current in superconductors enables the control of spins and magnetization without dissipation [1–3]—a critical functionality in realizing low-power spintronics [4–6]. Microscopically, this process occurs through the superconducting magnetolectric effect (sometimes known as the Edelstein effect) [2, 3, 7–14], where a supercurrent flowing through a noncentrosymmetric metal can induce a net magnetization of the carriers. In Rashba superconductors [15–17], such magnetolectric effects can be naturally understood through the spin-orbit interaction (SOI): spin readily couples to the motion of electrons (and their associated Cooper pairs) producing a net spin polarization in the presence of supercurrent flow.

Major attention has focused on the linear superconducting magnetolectric effect, where a spin response develops by driving supercurrent in time-reversal (\mathcal{T}) invariant noncentrosymmetric superconductors. For example, superconductors with a polar axis \mathbf{c} and Rashba SOI [2, 3] possess a supercurrent-induced magnetization $\mathbf{M} \propto \mathbf{c} \times \mathbf{J}_s$ that lies in-plane. Here \mathbf{J}_s is the supercurrent density. However, the nonlinear magnetolectric effect in superconductors is much less studied. Indeed, even in the normal state, nonlinear spin generation is a topic of intense recent interests [18–22].

In this work, we unveil the nonlinear superconducting magnetolectric effect (NSM) by examining second-order spin generation in response to the supercurrent. Specifically, we find a (second-order nonlinear) supercurrent-induced magnetization $\delta\mathbf{M}$ in two dimensions as

$$\delta M_c^{(2)} = \chi_{ab}^c q_a q_b, \quad (1)$$

where $a, b = x, y$ is the direction of the supercurrent, $c = x, y, z$, and \mathbf{q} is the Cooper pair momentum in the presence of supercurrent flow. Note χ_{ab}^c vanishes in the presence of \mathcal{T} symmetry. As a result, to realize the second-order nonlinear response, \mathcal{T} symmetry breaking is necessary. Interestingly, Eq. (1) persists even in cen-

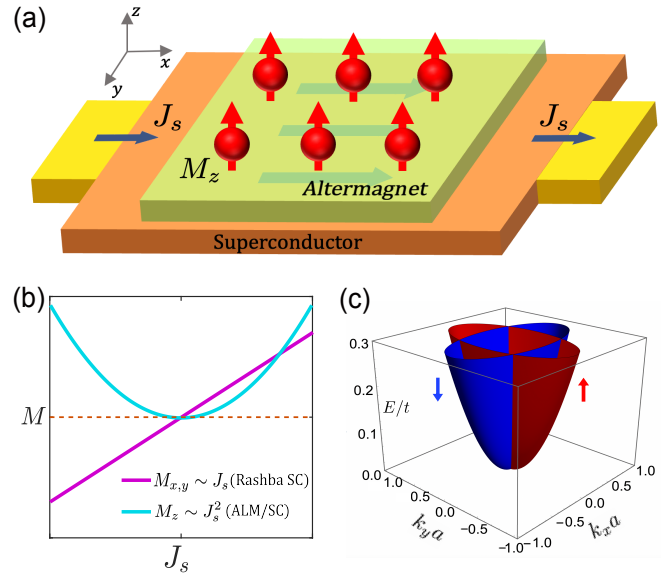


FIG. 1. (a) Schematic illustration of the ALM/SC heterostructure exhibiting the nonlinear superconducting magnetolectric (NSM) effect. In the presence of a supercurrent J_s flowing along x direction, the net magnetization along z direction M_z can be created. (b) In noncentrosymmetric superconductors with Rashba SOI, an in-plane magnetization, denoted as $M_{x,y}$, that is linear with J_s can be generated. In ALM/SC heterostructures, an out-of-plane M_z is generated that goes as J_s^2 . When $J_s = 0$, $M_z = 0$ in the ALM/SC heterostructure vanishes due to $C_4\mathcal{T}$ symmetry. (c) The normal-state band structure of the altermagnet from Eq. (8) at $J_{\text{ex}} = 0.4t$. The spin-split bands for spin \uparrow and spin \downarrow are indicated in red and blue respectively.

trosymmetric systems in sharp contrast to the case of the linear magnetolectric effect in noncentrosymmetric superconductors [9]. As we argue, NSM can be naturally realized in magnet/superconductor heterostructures by utilizing the proximity effect between a magnetic material and an s -wave superconductor [8, 23–25].

For concreteness, we propose an altermagnet/superconductor (ALM/SC) heterostructure as depicted in Fig. 1(a) as a natural candidate for NSM. Altermagnets are collinear antiferromagnets with unconventional magnetic order [26–36]; recently, several potential altermagnetic materials have been identified by *ab initio* simulations [26–28]. A characteristic property of *d*-wave altermagnets is $C_4\mathcal{T}$ symmetry, which breaks \mathcal{T} and four-fold rotational (C_4) symmetry individually but preserve the combination of them. The interplay between the altermagnets and superconductivity has been theoretically investigated [37–43].

For ALM/SC heterostructures, we find that a nonvanishing out-of-plane spin magnetization can be generated in the second-order response to the driving supercurrent. This is in sharp contrast to the case of polar or gyrotropic superconductors [2, 9, 13]. This work is organized as follows: First we present a general theory of supercurrent-induced spin generation including both the linear (first order) and nonlinear (second order) terms. Then we focus on the case in a specific ALM/SC realization. Remarkably, due to $C_4\mathcal{T}$ symmetry in altermagnets, we find that the second-order response χ_{ab}^z provides the leading order contribution to the out-of-plane spin magnetization; both equilibrium out-of-plane magnetization and linear-order out-of-plane magnetoelectric effects vanish. Additionally, due to the presence of a weak SOI in real altermagnets, the linear magnetoelectric effect also shows up in the in-plane direction. Furthermore, in the weak oscillating regime, driving an AC supercurrent can induce the second harmonic and rectified magnetization. Finally, we discuss possible material candidates that include thin films of the altermagnet RuO_2 and KRu_4O_8 on an *s*-wave superconductor. We propose that ALM/SC devices allow for the non-dissipative electric control of magnetization, which is important for high density magnetic memories and offers tantalizing possibilities for spin transport in which Joule heating and dissipation are minimized.

Superconducting magnetoelectric effect—We first examine the superconducting magnetoelectric effect within an effective Bogoliubov-de Gennes (BdG) framework. We note that our treatment is general and is agnostic to the precise microscopics of the superconducting gap: the superconducting state can be intrinsic or proximity induced. In what follows, we describe either case phenomenologically via the pairing potential $\hat{\Delta}_{\mathbf{k}}$. The finite- \mathbf{q} BdG Hamiltonian in the Nambu basis $(\hat{c}_{\mathbf{k}+\mathbf{q}/2,\uparrow}, \hat{c}_{\mathbf{k}+\mathbf{q}/2,\downarrow}, \hat{c}_{-\mathbf{k}+\mathbf{q}/2,\uparrow}^\dagger, \hat{c}_{-\mathbf{k}+\mathbf{q}/2,\downarrow}^\dagger)$ reads

$$\mathcal{H}_{\text{BdG}}^{\mathbf{k},\mathbf{q}} = \begin{pmatrix} H_{\mathbf{k}+\mathbf{q}/2} & \hat{\Delta}_{\mathbf{k}} \\ \hat{\Delta}_{\mathbf{k}}^\dagger & -H_{-\mathbf{k}+\mathbf{q}/2}^* \end{pmatrix}, \quad (2)$$

where $H_{\mathbf{k}}$ is the Bloch Hamiltonian of the normal state, and \mathbf{q} is the momentum of the Cooper pair. As we will see below, altermagnetic $H_{\mathbf{k}}$ enables the NSM effect. For

TABLE I. Symmetry restrictions for three components of \mathbf{M} in a two-dimensional system. Note that $C_4\mathcal{T}$ corresponds to the case for altermagnets that we focus on in our work. 1(2) indicates first (second) order response. \checkmark indicates allowed and \times indicates forbidden.

	\mathcal{P}	\mathcal{T}	\mathcal{PT}	$C_4\mathcal{T}$
M_x	$\checkmark(2)$	$\checkmark(1)$	\times	$\checkmark(1)$
M_y	$\checkmark(2)$	$\checkmark(1)$	\times	$\checkmark(1)$
M_z	$\checkmark(2)$	$\checkmark(1)$	\times	$\checkmark(2)$

simplicity we have used a \mathbf{q} -independent gap function $\hat{\Delta}_{\mathbf{k}}$, which is valid for weak values of the applied current [12].

The total free energy \mathcal{F} of the ALM/SC heterostructure comprises two parts: the superconductor component \mathcal{F}_{sc} and the material (i.e. altermagnet) component \mathcal{F}_{al} so that $\mathcal{F} = \mathcal{F}_{\text{sc}} + \mathcal{F}_{\text{al}}$. The supercurrent can be tracked as $\mathbf{J}_s = \nu_s \mathbf{q}$ with the condensate superfluid stiffness $\nu_s = \partial^2 \mathcal{F}_{\text{sc}}(\mathbf{q}) / \partial^2 \mathbf{q}$. As a result, observables that scale with q below are induced by the supercurrent at linear order while q^2 indicates a second-order nonlinear response.

The magnetic response of the heterostructure can be obtained in the standard fashion by analyzing the set of parametric partition function $\mathcal{Z}(\mathbf{h})$

$$\mathcal{Z}(\mathbf{h}) = e^{-\beta \{ \mathcal{F}_{\text{sc}} - \frac{1}{2\beta} \sum_{\mathbf{k},\mathbf{q},n} \text{Tr}[\log G^{-1}(\mathbf{k},\mathbf{q},\mathbf{h},i\omega_n)] \}}, \quad (3)$$

where \mathbf{h} is a parameter describing an auxiliary Zeeman field with a corresponding Zeeman energy $\Sigma(\mathbf{h}) = \text{diag}(g_s \mu_B \mathbf{h} \cdot \hat{s}, -g_s \mu_B \mathbf{h} \cdot \hat{s}^*) / 2$. Here $g_s = 2$ is the Landé *g* factor, μ_B being the Bohr magneton, and the Gor'kov's Green's functions are $G^{-1}(\mathbf{k},\mathbf{q},\mathbf{h},i\omega_n) = \mathcal{G}^{-1}(\mathbf{k},\mathbf{q},i\omega_n) + \Sigma(\mathbf{h})$ and $\mathcal{G}(\mathbf{k},\mathbf{q},i\omega_n) = (i\omega_n - \mathcal{H}_{\text{BdG}}^{\mathbf{k},\mathbf{q}})^{-1}$ with the Matsubara frequency $\omega_n = (2n+1)\pi/\beta$. $\beta = 1/k_B T$ with T being the temperature.

The spin magnetization can be evaluated as $\mathbf{M} = -\beta^{-1} \partial \log \mathcal{Z}(\mathbf{h}) / \partial \mathbf{h}|_{\mathbf{h}=0}$. Using the BdG Hamiltonian [Eq. (2)] in the current-carrying state, we obtain the spin magnetization as

$$M_a = -\frac{g_s \mu_B}{4\beta} \sum_{n\mathbf{k}} \text{Tr}[\mathcal{G}(\mathbf{k},\mathbf{q},i\omega_n) \eta_a]. \quad (4)$$

Here $\eta_a = \text{diag}(s_a, -s_a^*)$ are the generalized spin Pauli matrices in the Nambu space. To extract the linear and nonlinear responses systematically, we expand the BdG Hamiltonian as

$$\mathcal{H}_{\text{BdG}}^{\mathbf{k},\mathbf{q}} = \mathcal{H}_{\text{BdG}}^{\mathbf{k},\mathbf{q}=0} + \frac{1}{2} q_a \hat{v}_a + \frac{1}{8} q_a q_b \hat{w}_{ab}, \quad (5)$$

where $\hat{v}_a = \text{diag}[\mathcal{V}_a(\mathbf{k}), -\mathcal{V}_a^*(-\mathbf{k})]$ and $\hat{w}_{ab} = \text{diag}[\mathcal{W}_{ab}(\mathbf{k}), -\mathcal{W}_{ab}^*(-\mathbf{k})]$ with $\mathcal{V}_a(\mathbf{k}) = \partial H_{\mathbf{k}} / \partial k_a$ and $\mathcal{W}_{ab}(\mathbf{k}) = \partial^2 H_{\mathbf{k}} / \partial k_a \partial k_b$. At linear order in \mathbf{q} , we find

$\delta M_a^{(1)} = \alpha_{ab} q_b$, where the first-order spin susceptibility α_{ab} reads

$$\alpha_{ab} = -\frac{g_s \mu_B}{8\beta} \sum_{n\mathbf{k}} \text{Tr}[\eta_a \mathcal{G}_0 \hat{v}_b \mathcal{G}_0], \quad (6)$$

where $\mathcal{G}_0 \equiv \mathcal{G}(\mathbf{k}, 0, i\omega_n) = (i\omega_n - \mathcal{H}_{\text{BdG}}^{\mathbf{k}, q=0})^{-1}$ for brevity. This formula is consistent with the results in Ref. [12]. Importantly, we find the nonlinear spin magnetization along c direction in Eq. (1) with the second-order spin susceptibility χ as

$$\chi_{ab}^c = -\frac{g_s \mu_B}{32\beta} \sum_{n\mathbf{k}} \text{Tr}[\eta_c (\mathcal{G}_0 \hat{v}_a \mathcal{G}_0 + 2\mathcal{G}_0 \hat{v}_a \mathcal{G}_0 \hat{v}_b \mathcal{G}_0)]. \quad (7)$$

We note that that χ_{ab}^c in Eq. (7) is *general* for arbitrary model Bloch Hamiltonians as well as pairing potentials. In particular, Eq. (7) applies for both conventional pairing as well as unconventional pairing $\hat{\Delta}_{\mathbf{k}}$. However, in the next section we will take a simple s -wave pairing $\hat{\Delta}_{\mathbf{k}} = \Delta_0 i s_y$ with a \mathbf{k} -independent pairing gap as an illustrative example to emphasize the effect of the magnetic order. Detailed derivations can be found in Supplementary Material [44].

It is instructive to examine the symmetry requirements for both the linear α_{ab} and second-order NSM χ_{ab}^c summarized in Table I. For instance, \mathcal{T} breaking is necessary for non-zero χ_{ab}^c while \mathcal{P} breaking is necessary for α_{ab} ; both are destroyed in \mathcal{PT} -invariant systems. A particular interesting case is that of $C_4\mathcal{T}$ symmetry found in altermagnets: we find that χ_{ab}^x and χ_{ab}^y terms vanish; only χ_{ab}^z is non-zero. Interestingly, $C_4\mathcal{T}$ further constrains the NSM so that $\chi_{xx}^z = -\chi_{yy}^z$. In the presence of a weak SOI naturally found in realistic altermagnets, in-plane spin magnetization can be induced as expected of a linear magnetoelectric effect in Eq. (6). Importantly, however, the Rashba SOI induced linear magnetoelectric effect is purely in-plane ($\alpha_{zx} = \alpha_{zy} = 0$). This means that for out-of-plane magnetization responses, the second order NSM χ_{ab}^z is the leading order term in the altermagnetic systems. As we will see below, it dominates the out-of-plane magnetization responses.

NSM in ALM/SC heterostructure—In the set-up illustrated in Fig. 1(a), an altermagnet thin film is in contact with a conventional s -wave superconductor. To characterize the physics of quasi-2D planar $d_{x^2-y^2}$ -wave altermagnet, we adopt a generic two-band Hamiltonian [27], yielding

$$H_{\mathbf{k}} = [ta^2(k_x^2 + k_y^2) - \mu]s_0 + J_{\text{ex}}a^2(k_x^2 - k_y^2)s_z. \quad (8)$$

Here t parameterizes the usual kinetic energy, J_{ex} denotes the $d_{x^2-y^2}$ exchange magnetic order and μ is the Fermi energy. a denotes the lattice constant. We note that an additional Rashba SOI term $H_R = \lambda a(k_x s_y - k_y s_x)$ can be readily added to $H_{\mathbf{k}}$ with λ term representing the strength of SOI, that arises in altermagnets [27, 35].

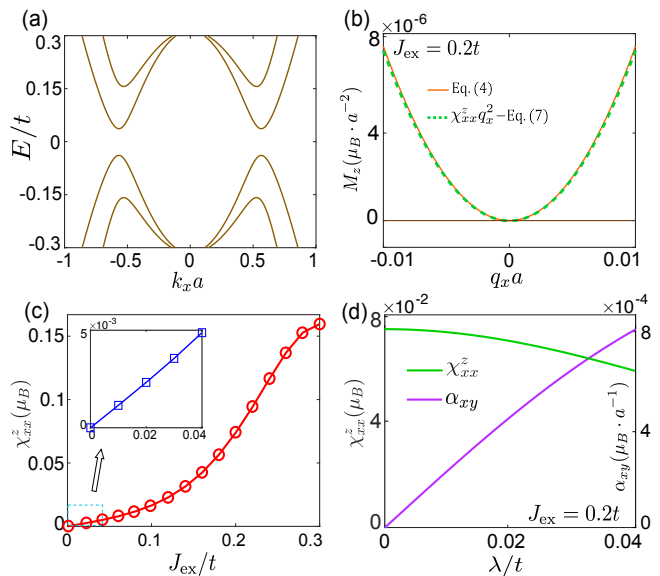


FIG. 2. (a) The fully gapped BdG energy spectrum of ALM/SC from Eq. (2) with Bloch Hamiltonian in Eq. (8) at $k_y = 0$ using a phenomenological gap $\hat{\Delta}_{\mathbf{k}} = \Delta_0 i s_y$. (b) The spin magnetization M_z as a function of q_x from Eq. (4) (solid orange). As a comparison, the NSM susceptibility multiplied by q_x^2 is plotted as Eq. (7) (dashed green). (c) The nonlinear spin susceptibility χ_{xx}^z as a function of d -wave magnetic order J_{ex} . The inset shows the region of $0 < J_{\text{ex}} < 0.04t$. (d) For nonzero λ , the linear and nonlinear spin susceptibilities α_{xy} and χ_{xx}^z as a function of λ . α_{xy} increases linearly with λ for small λ . Parameters: $\lambda = 0$ for (a), (b) and (c). $J_{\text{ex}} = 0.2t$ for (a), (b) and (d). $(\Delta_0, \mu) = (0.1, 0.3)t$ for all four panels. The temperature is set to be $T = 0.3T_c$.

Here, s matrices operate on the spin degree of freedom. This Hamiltonian breaks time reversal symmetry $\mathcal{T} = -i s_y \mathcal{K}$ (\mathcal{K} is the complex conjugate) and four-fold rotation symmetry $C_4 = e^{i\pi s_z/4}$, but preserves the combination of them as $C_4\mathcal{T}$. The SOI term breaks inversion (\mathcal{P}) symmetry without breaking $C_4\mathcal{T}$. Throughout our work, we use the energy unit t . As an illustration of the spin-split band structure in altermagnet, we plot Eq. (8) in Fig. 1(c); here we have used $J_{\text{ex}} = 0.4t$ and $\lambda = 0$.

Because of the proximity effect between the altermagnet and superconductor, Cooper pairs can tunnel into the altermagnet. For a thin film of altermagnet [see Fig. 1(a)], with thickness d much less than the coherence length of the superconductor ($d \ll \xi$), the pairing gap is approximately uniform along the z direction. We have focused on an conventional s -wave superconductor with the pairing Δ_0 . Using the parameters as $(J_{\text{ex}}, \lambda, \mu, \Delta_0) = (0.2, 0, 0.3, 0.1)t$, we diagonalize the BdG Hamiltonian and plot the fully gapped BdG energy spectrum in Fig. 2(a). Although the pairing potential is purely s -wave, the induced superconducting correlations can be obtained as $F = [\psi_0 + \mathbf{d}(\mathbf{k}) \cdot \mathbf{s}] i s_y$, where ψ_0 and \mathbf{d} vector parameterize the spin-singlet and spin-

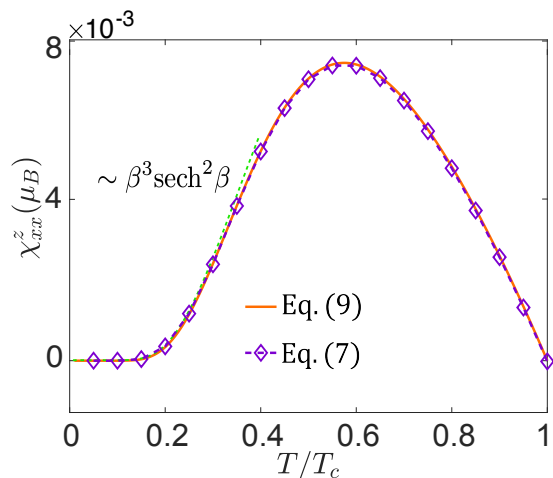


FIG. 3. The second-order spin susceptibility χ_{xx}^z as a function of the temperature T at $(J_{\text{ex}}, \Delta_0, \mu) = (0.02, 0.1, 0.3)t$. The purple diamonds denotes the numerical results from Eq. (7) and the orange line denotes the analytical result from Eq. (9). At low temperatures, $\chi_{xx}^z \sim \beta^3 \text{sech}^2 \beta$.

triplet pairing correlations, respectively [45–47]. We have $d = (0, 0, d_z)$ with $d_z \propto J_{\text{ex}}(k_x^2 - k_y^2)$, indicating that the d -wave magnetic order gives rise to the spin-triplet pairing correlation in altermagnets due to the proximity effect.

To illustrate NSM effect in the ALM/SC heterostructure, we numerically study the supercurrent induced magnetization in Fig. 2 for the Bloch Hamiltonian in Eq. (8). By applying the current along x direction as $\mathbf{q} = (q_x, 0)$, we calculate the magnetization directly from Eq. (4) at $J_{\text{ex}} = 0.2t$ as shown in Fig. 2(b). One finds that $M_z \sim q_x^2$ as expected from Fig. 1(b). It is also worth noting that when $q_x = 0$, equilibrium magnetization vanishes $M_z = 0$, which is consistent with $C_4\mathcal{T}$ symmetry in altermagnets. We note that numerically computing the NSM susceptibility χ_{xx}^z from Eq. (7) and multiplying by q_x^2 as plotted in the dashed green line matches the solid line in orange [from Eq. (4)].

In Fig. 2(c), we show the second-order spin susceptibility χ_{xx}^z as a function of J_{ex} from Eq. (7). Generally, χ_{xx}^z starts to grow linearly with J_{ex} as shown in the zoom-in inset of Fig. 2(c). Furthermore, we also calculate the first-order spin susceptibility α_{xy} (purple) which is shown in Fig. 2(d). As expected, α_{xy} directly depends on λ ; for small λ , α_{xy} increases linearly with λ and vanishes when $\lambda = 0$. In contrast, for NSM χ_{xx}^z is finite for $\lambda = 0$ and exhibits a weak dependence on λ ; χ_{xx}^z becomes smaller when λ is nonzero since Rashba SOI tends to pin the spin in the in-plane direction and weakens the out-of-plane spin polarization. In our calculations, we adopt the BCS temperature dependence (for the s -wave superconductor substrate) of Δ_0 with $\Delta(T) = \Delta_0 \tanh(1.74\sqrt{T_c/T} - 1)$ and $\Delta_0 = 1.76k_B T_c$.

In contrast to the linear magnetoelectric effect in

Rashba-type superconductors, we find that the temperature dependence of NSM spin generation is non-monotonic. Expanding in small $J_{\text{ex}} \ll t$, we can obtain an approximate analytical result for the temperature dependence of χ_{xx}^z as $\chi_{xx}^z = \mu_B \int_0^\infty f(x) dx + \mathcal{O}(J_{\text{ex}}^2)$ with

$$f(x) = \frac{\beta^3 J_{\text{ex}}}{64\pi} x \text{sech}^2 \gamma \left[\frac{4}{\beta^2} + t^2 x^4 (2 - 3 \text{sech}^2 \gamma) + \frac{4tx^2(\mu - tx^2) \tanh \gamma}{\gamma} \right], \quad (9)$$

where $\gamma = \beta \sqrt{\Delta(T)^2 + (tx^2 - \mu)^2} / 2$. By employing Eq. (9), we plot the χ_{xx}^z as a function of temperature in Fig. 3 (orange solid curve) with $J_{\text{ex}} = 0.02t$. By way of comparison, we also show a fully numerical plot of Eq. (7) (purple diamonds); both agree with each other. Interestingly, χ_{xx}^z vanishes at zero temperature. At low temperatures ($\beta\Delta_0 \gg 1$), χ_{xx}^z starts to grow with T scaling as $\chi_{xx}^z \sim \beta^3 \text{sech}^2 \beta$. However, at $T/T_c \sim 0.6$, it reaches a peak after which it rapidly diminishes with temperature. This non-monotonic behavior contrasts sharply with that of the linear magnetoelectric effect in Rashba-type superconductors [13, 44] that instead saturates at low temperature.

In superconductors, supercurrent flow can arise due to either an external applied magnetic field or an explicit transport current [48]. In the former case, there is a screening supercurrent on the surface of the superconductor. In the latter case, the global excitation of the superconductor gives a uniform Cooper pair momentum \mathbf{q} . Specifically, for slowly varying AC supercurrent as $\mathbf{J}_s(t) = \mathbf{J}_\omega \cos \omega t$ with $\omega \ll \Delta_0$, we expect an oscillatory Cooper pair momentum $\mathbf{q}(t) = \mathbf{q}_\omega \cos \omega t$. This will allow to obtain a second harmonic magnetization in the weak oscillating regime with $\chi_{ab}^c(2\omega) = \chi_{ab}^c/4$.

Candidate materials.—We anticipate that NSM we discuss here can be realized in ALM/SC formed out of readily available d -wave altermagnetic materials [27]. As an example, consider the altermagnet RuO_2 with in-plane lattice constant $a = 4.5\text{\AA}$, and $t = 2.5$ eV, $J_{\text{ex}} = 0.5$ eV [32, 39]. Using a pairing gap of $\Delta_0 = 1$ meV, $\mu = 10$ meV, $\lambda = 10$ meV and $T = 0.3T_c$ we estimate $\chi_{xx}^z \approx 0.07\mu_B$. For a Cooper pair momentum $q \approx 10^{-3}\text{\AA}^{-1}$ [49], the induced out-of-plane spin density in the RuO_2 thin film/superconductor heterostructure is $\sim 0.7 \times 10^{-5} \mu_B/\text{nm}^2$. Note that this value is comparable to the spin generation in MnBi_2Te_4 and other noncentrosymmetric ferromagnetic systems [19, 50, 51]. Another example is KRu_4O_8 with the parameter values: $t = 0.05$ eV, $J_{\text{ex}} = 0.018$ eV, and $a = 9.9\text{\AA}$. We find $\chi_{xx}^z \approx 0.01\mu_B$ and out-of-plane spin density similar to that discussed above. These magnitudes are estimated qualitatively using a low-energy effective description of altermagnets in the small J and weak doping (small μ) regime as well as a gapped BdG spectrum. In real altermagnets with large J and high doping, the BdG spectrum

becomes gapless. We anticipate this may enhance NSM with additional contribution from the quasiparticles excited at finite temperature.

In this work, we have proposed a novel nonlinear superconducting magnetoelectric effect. Naturally occurring in ALM/SC heterostructures, this second-order spin generation in response to the supercurrent becomes the leading order contribution to the magnetization along the out-of-plane direction. Supercurrent induced magnetization can be readily detected by using a superconducting quantum interference device (SQUID) perpendicular to the altermagnet surface, which can be employed to probe the magnetic flux change [12]. Interestingly, nonlinear spin generation that is second order in an applied electric field can be realized in normal-state (non-superconducting) altermagnets with $C_4\mathcal{T}$ symmetry [19]. Our work shows that nonlinear spin generation survives in the superconducting state and is driven by a dissipationless supercurrent.

Acknowledgements.—We thank Bo Yang and Wen-Yu He for helpful discussions. This work was supported by the Ministry of Education Singapore under its Academic Research Fund Tier 2 Grant No. MOE-T2EP50222-0011.

Note added.—Recently, we became aware of an independent pre-print posted on the arXiv in Ref. [52] which also found a second-order supercurrent-induced spin polarization in superconductors with d -wave magnetization.

* jinxin.hu@ntu.edu.sg

† justinsong@ntu.edu.sg

- [1] L. Levitov, Y. V. Nazarov, and G. Eliashberg, *Soviet Journal of Experimental and Theoretical Physics* **61**, 133 (1985).
- [2] V. M. Edelstein, *Physical review letters* **75**, 2004 (1995).
- [3] V. M. Edelstein, *Physical Review B* **72**, 172501 (2005).
- [4] J. Linder and J. W. Robinson, *Nature Physics* **11**, 307 (2015).
- [5] M. Eschrig, *Reports on Progress in Physics* **78**, 104501 (2015).
- [6] M. Eschrig, *Physics Today* **64**, 43 (2011).
- [7] S. Fujimoto, *Physical Review B* **72**, 024515 (2005).
- [8] G. Tkachov, *Physical review letters* **118**, 016802 (2017).
- [9] W.-Y. He and K. T. Law, *Physical Review Research* **2**, 012073 (2020).
- [10] W.-Y. He and K. T. Law, *Physical Review Research* **3**, L032012 (2021).
- [11] Y. Ikeda and Y. Yanase, *Physical Review B* **102**, 214510 (2020).
- [12] L. Chirulli, M. T. Mercaldo, C. Guarcello, F. Giazotto, and M. Cuoco, *Physical Review Letters* **128**, 217703 (2022).
- [13] J. J. He, K. Hiroki, K. Hamamoto, and N. Nagaosa, *Communications Physics* **2**, 128 (2019).
- [14] N. F. Yuan, arXiv preprint arXiv:2311.11087 (2023).
- [15] E. Bauer and M. Sigrist, *Non-centrosymmetric superconductors: introduction and overview*, Vol. 847 (Springer Science & Business Media, 2012).
- [16] M. Smidman, M. Salamon, H. Yuan, and D. Agterberg, *Reports on Progress in Physics* **80**, 036501 (2017).
- [17] M. Houzet and J. S. Meyer, *Physical Review B* **92**, 014509 (2015).
- [18] K. Hamamoto, M. Ezawa, K. W. Kim, T. Morimoto, and N. Nagaosa, *Physical Review B* **95**, 224430 (2017).
- [19] C. Xiao, H. Liu, W. Wu, H. Wang, Q. Niu, and S. A. Yang, *Physical Review Letters* **129**, 086602 (2022).
- [20] C. Xiao, W. Wu, H. Wang, Y.-X. Huang, X. Feng, H. Liu, G.-Y. Guo, Q. Niu, and S. A. Yang, *Physical Review Letters* **130**, 166302 (2023).
- [21] R. Guo, Y.-X. Huang, X. Yang, Y. Liu, C. Xiao, and Z. Yuan, arXiv preprint arXiv:2402.07756 (2024).
- [22] X. Feng, W. Wu, H. Wang, W. Gao, L. K. Ang, Y. Zhao, C. Xiao, and S. A. Yang, arXiv preprint arXiv:2402.00532 (2024).
- [23] L. Fu and C. L. Kane, *Physical review letters* **100**, 096407 (2008).
- [24] X.-L. Qi, T. L. Hughes, and S.-C. Zhang, *Physical Review B* **82**, 184516 (2010).
- [25] J. Wang, Q. Zhou, B. Lian, and S.-C. Zhang, *Physical Review B* **92**, 064520 (2015).
- [26] H.-Y. Ma, M. Hu, N. Li, J. Liu, W. Yao, J.-F. Jia, and J. Liu, *Nature communications* **12**, 2846 (2021).
- [27] L. Šmejkal, J. Sinova, and T. Jungwirth, *Physical Review X* **12**, 040501 (2022).
- [28] S. Lee, S. Lee, S. Jung, J. Jung, D. Kim, Y. Lee, B. Seok, J. Kim, B. G. Park, L. Šmejkal, *et al.*, *Physical Review Letters* **132**, 036702 (2024).
- [29] I. Mazin *et al.*, *Physical Review X* **12**, 040002 (2022).
- [30] I. Mazin, *Physical Review B* **107**, L100418 (2023).
- [31] Z. Feng, X. Zhou, L. Šmejkal, L. Wu, Z. Zhu, H. Guo, R. González-Hernández, X. Wang, H. Yan, P. Qin, *et al.*, *Nature Electronics* **5**, 735 (2022).
- [32] L. Šmejkal, A. B. Hellenes, R. González-Hernández, J. Sinova, and T. Jungwirth, *Physical Review X* **12**, 011028 (2022).
- [33] L. Šmejkal, A. Marmodoro, K.-H. Ahn, R. González-Hernández, I. Turek, S. Mankovsky, H. Ebert, S. W. D'Souza, O. Šipr, J. Sinova, *et al.*, *Physical Review Letters* **131**, 256703 (2023).
- [34] S. A. A. Ghorashi, T. L. Hughes, and J. Cano, arXiv preprint arXiv:2306.09413 (2023).
- [35] Y. Fang, J. Cano, and S. A. A. Ghorashi, arXiv preprint arXiv:2310.11489 (2023).
- [36] J. Krempaský, L. Šmejkal, S. D'Souza, M. Hajlaoui, G. Springholz, K. Uhlířová, F. Alarab, P. Constantinou, V. Strocov, D. Usanov, *et al.*, *Nature* **626**, 517 (2024).
- [37] D. Zhu, Z.-Y. Zhuang, Z. Wu, and Z. Yan, *Physical Review B* **108**, 184505 (2023).
- [38] C. Beenakker and T. Vakhel, *Physical Review B* **108**, 075425 (2023).
- [39] S.-B. Zhang, L.-H. Hu, and T. Neupert, *Nature Communications* **15**, 1801 (2024).
- [40] J. A. Ouassou, A. Brataas, and J. Linder, *Physical Review Letters* **131**, 076003 (2023).
- [41] M. Papaj, *Physical Review B* **108**, L060508 (2023).
- [42] Y.-X. Li and C.-C. Liu, *Physical Review B* **108**, 205410 (2023).
- [43] H. G. Giil, B. Brekke, J. Linder, and A. Brataas, arXiv preprint arXiv:2403.04851 (2024).
- [44] See Supplemental Material for 1. Theory of nonlinear superconducting magnetoelectric effect; 2. Pairing correlations; 3. Linear Edelstein effect in Rashba-type supercon-

ductors.

- [45] L. P. Gor'kov and E. I. Rashba, Physical Review Letters **87**, 037004 (2001).
- [46] P. Frigeri, D. Agterberg, A. Koga, and M. Sigrist, Physical review letters **92**, 097001 (2004).
- [47] B. T. Zhou, N. F. Yuan, H.-L. Jiang, and K. T. Law, Physical Review B **93**, 180501 (2016).
- [48] A. Anthore, H. Pothier, and D. Esteve, Physical review letters **90**, 127001 (2003).
- [49] Z. Zhu, M. Papaj, X.-A. Nie, H.-K. Xu, Y.-S. Gu, X. Yang, D. Guan, S. Wang, Y. Li, C. Liu, *et al.*, Science **374**, 1381 (2021).
- [50] A. Chernyshov, M. Overby, X. Liu, J. K. Furdyna, Y. Lyanda-Geller, and L. P. Rokhinson, Nature Physics **5**, 656 (2009).
- [51] D. Fang, H. Kurebayashi, J. Wunderlich, K. Vybörný, L. P. Zárbo, R. Champion, A. Casiraghi, B. Gallagher, T. Jungwirth, and A. Ferguson, Nature nanotechnology **6**, 413 (2011).
- [52] A. A. Zyuzin, arXiv preprint arXiv:2402.15459 (2024).

Supplementary Material for “Nonlinear Superconducting Magnetoelectric Effect”

Jin-Xin Hu,¹ Oles Matsyshyn,¹ Justin C. W. Song¹

¹*Division of Physics and Applied Physics, School of Physical and Mathematical Sciences, Nanyang Technological University, Singapore 637371*

I. THEORY OF NONLINEAR SUPERCONDUCTING MAGNETOELECTRIC EFFECT

A. Green’s function method

In this section we provide more details for deriving the general formula of superconducting magnetoelectric effect, including both the linear and nonlinear terms. The superconducting state can be intrinsic or proximity induced with a pairing function $\hat{\Delta}_{\mathbf{k}}$. $\hat{\Delta}_{\mathbf{k}}$ can be conventional s -wave with a uniform pairing gap $\hat{\Delta}_{\mathbf{k}} = \Delta_0 i s_y$ or unconventional pairing states. In the current-carrying state, the finite- \mathbf{q} Bogoliubov-de Gennes (BdG) Hamiltonian in the Nambu basis $(\hat{c}_{\mathbf{k}+\mathbf{q}/2,\uparrow}, \hat{c}_{\mathbf{k}+\mathbf{q}/2,\downarrow}, \hat{c}_{-\mathbf{k}+\mathbf{q}/2,\uparrow}^\dagger, \hat{c}_{-\mathbf{k}+\mathbf{q}/2,\downarrow}^\dagger)$ reads

$$\mathcal{H}_{\text{BdG}}^{\mathbf{k},\mathbf{q}} = \begin{pmatrix} H_{\mathbf{k}+\mathbf{q}/2} & \hat{\Delta}_{\mathbf{k}} \\ \hat{\Delta}_{\mathbf{k}}^\dagger & -H_{-\mathbf{k}+\mathbf{q}/2}^* \end{pmatrix} \quad (\text{S1})$$

where $H_{\mathbf{k}}$ is the Bloch Hamiltonian of the normal state, \mathbf{q} is the momentum of the Cooper pair, and s_y is a Pauli matrix. For simplicity we have used a \mathbf{q} -independent gap function $\hat{\Delta}_{\mathbf{k}}$, which is valid for weak values of the applied current.

In the main text, we focus on the altermagnet/superconductor heterostructure. The total free energy \mathcal{F} of the system contains the superconductor part \mathcal{F}_{sc} and the altermagnet part \mathcal{F}_{al} with $\mathcal{F} = \mathcal{F}_{\text{sc}} + \mathcal{F}_{\text{al}}$. The supercurrent $J_s = \nu_s \mathbf{q}$ with the superfluid density $\nu_s = \partial^2 \mathcal{F}_{\text{sc}}(\mathbf{q}) / \partial^2 \mathbf{q}$. The partition function $\mathcal{Z}(\mathbf{h})$ is given by

$$\mathcal{Z}(\mathbf{h}) = e^{-\beta[\mathcal{F}_{\text{sc}} - \frac{1}{2\beta} \sum_{\mathbf{k},\mathbf{q},n} \text{Tr}[\log G^{-1}(\mathbf{k},\mathbf{q},\mathbf{h},i\omega_n)]]}. \quad (\text{S2})$$

By introducing an auxiliary Zeeman field \mathbf{h} , we can write down the modified BdG Hamiltonian:

$$\mathcal{H}_{\text{BdG}}^{\mathbf{k},\mathbf{q}}(\mathbf{h}) = \begin{pmatrix} H_{\mathbf{k}+\mathbf{q}/2} - \frac{1}{2} g_s \mu_B \mathbf{h} \cdot \mathbf{s} & \hat{\Delta}_{\mathbf{k}} \\ \hat{\Delta}_{\mathbf{k}}^\dagger & -H_{-\mathbf{k}+\mathbf{q}/2}^* + \frac{1}{2} g_s \mu_B \mathbf{h} \cdot \mathbf{s}^* \end{pmatrix}, \quad (\text{S3})$$

This auxiliary Zeeman field is to be distinguished from the genuine magnetization of the system and is set to zero at the end of the calculation. The Gor’kov’s Green’s function is $G(\mathbf{k}, \mathbf{q}, \mathbf{h}, i\omega_n) = [i\omega_n - \mathcal{H}_{\text{BdG}}^{\mathbf{k},\mathbf{q}}(\mathbf{h})]^{-1}$. The magnetization M can be obtained from the partition function as

$$\begin{aligned} M_a &= -\frac{1}{\beta} \frac{\partial}{\partial h_a} \log Z(\mathbf{h}) \\ &= -\frac{1}{2\beta} \sum_{\mathbf{k},\mathbf{q},n} \frac{\partial}{\partial h_a} \text{Tr}[\log G^{-1}(\mathbf{k}, \mathbf{q}, \mathbf{h}, i\omega_n)] \end{aligned} \quad (\text{S4})$$

We decompose the Green’s function as $G^{-1}(\mathbf{k}, \mathbf{q}, \mathbf{h}, i\omega_n) = \mathcal{G}^{-1}(\mathbf{k}, \mathbf{q}, i\omega_n) + \Sigma(\mathbf{h})$ with

$$\Sigma(\mathbf{h}) = \begin{pmatrix} \frac{1}{2} g_s \mu_B \mathbf{h} \cdot \mathbf{s} & 0 \\ 0 & -\frac{1}{2} g_s \mu_B \mathbf{h} \cdot \mathbf{s} \end{pmatrix}, \quad (\text{S5})$$

We can then expand the logarithm in the first order of \mathbf{h} as $\log G^{-1}(\mathbf{k}, \mathbf{q}, \mathbf{h}, i\omega_n) = \log \mathcal{G}^{-1}(\mathbf{k}, \mathbf{q}, i\omega_n) + \mathcal{G}(\mathbf{k}, \mathbf{q}, i\omega_n) \Sigma(\mathbf{h})$. Thus, we can then obtain the magnetization M as

$$M_a = -\frac{g_s \mu_B}{4\beta} \sum_{n\mathbf{k}} \text{Tr}[\mathcal{G}(\mathbf{k}, \mathbf{q}, i\omega_n) \eta_a]. \quad (\text{S6})$$

Here $\eta_a = \text{diag}(s_a, -s_a^*)$ is the redefined spin Pauli matrices in the Nambu space. The Gor'kov Green's function is $\mathcal{G}(\mathbf{k}, \mathbf{q}, i\omega_n) = (i\omega_n - \mathcal{H}_{\text{BdG}}^{\mathbf{k}, \mathbf{q}})^{-1}$ with the Matsubara frequency $\omega_n = (2n + 1)\pi k_B T$. T is the temperature. $g_s = 2$ is the Landé g factor and μ_B is the Bohr magneton. We can then expand the BdG Hamiltonian as

$$\mathcal{H}_{\text{BdG}}^{\mathbf{k}, \mathbf{q}} = \mathcal{H}_{\text{BdG}}^{\mathbf{k}} + q_a \hat{v}_a / 2 + q_a q_b \hat{w}_{ab} / 8 + \mathcal{O}(\mathbf{q}^3) \quad (\text{S7})$$

The velocity operators are

$$\hat{v}_a = \begin{pmatrix} \hat{\mathcal{V}}_a(\mathbf{k}) & 0 \\ 0 & -\hat{\mathcal{V}}_a^*(-\mathbf{k}) \end{pmatrix}, \hat{w}_{ab} = \begin{pmatrix} \mathcal{W}_{ab}(\mathbf{k}) & 0 \\ 0 & -\mathcal{W}_{ab}^*(-\mathbf{k}) \end{pmatrix}. \quad (\text{S8})$$

Here we introduce $\mathcal{V}_a(\mathbf{k}) = \partial H_{\mathbf{k}} / \partial k_a$ and $\mathcal{W}_{ab}(\mathbf{k}) = \partial^2 H_{\mathbf{k}} / \partial k_a \partial k_b$. We proceed in evaluating terms of Eq. (S7), we note that if A and B are matrices and $B \ll A$ ($B \sim \mathcal{O}(\mathbf{q})$), we can expand the matrix expression in small B as

$$(A + B)^{-1} = A^{-1} - A^{-1} B A^{-1} + A^{-1} B A^{-1} B A^{-1} + \mathcal{O}(B^3). \quad (\text{S9})$$

In the following we will apply Eq. (S9) to the full Green function in order to make an effective expansion around small \mathbf{q} . We obtain

$$\mathcal{G}(\mathbf{k}, \mathbf{q}, i\omega_n) = (i\omega_n - \mathcal{H}_{\text{BdG}}^{\mathbf{k}, \mathbf{q}})^{-1} = \mathcal{G}_0 + \frac{1}{2} q_a \mathcal{G}_0 \hat{v}_a \mathcal{G}_0 + q_a q_b \left(\frac{1}{8} \mathcal{G}_0 \hat{w}_{ab} \mathcal{G}_0 + \frac{1}{4} \mathcal{G}_0 \hat{v}_a \mathcal{G}_0 \hat{v}_b \mathcal{G}_0 \right) \quad (\text{S10})$$

Here $\mathcal{G}_0 \equiv \mathcal{G}(\mathbf{k}, i\omega_n) = (i\omega_n - \mathcal{H}_{\text{BdG}}^{\mathbf{k}})^{-1}$. We insert Eq. (S10) to Eq. (S6) to get the magnetization susceptibility at both linear- and (nonlinear) second-order. Firstly, the first-order spin susceptibility α_{ab} is described by $\delta M_a^{(1)} = \alpha_{ab} q_b$, where α_{ab} reads

$$\alpha_{ab} = -\frac{g_s \mu_B k_B T}{8} \sum_{n\mathbf{k}} \text{Tr}[\eta_a \mathcal{G}_0 \hat{v}_b \mathcal{G}_0]. \quad (\text{S11})$$

More importantly, we can write the second-order nonlinear spin magnetization along c direction as $\delta M_c^{(2)} = \chi_{ab}^c q_a q_b$, and the nonlinear susceptibility χ can be obtained as

$$\chi_{ab}^c = -\frac{g_s \mu_B k_B T}{32} \sum_{n\mathbf{k}} \text{Tr}[\eta_c (\mathcal{G}_0 \hat{w}_{ab} \mathcal{G}_0 + 2\mathcal{G}_0 \hat{v}_a \mathcal{G}_0 \hat{v}_b \mathcal{G}_0)]. \quad (\text{S12})$$

B. Analytical result

In the previous subsection, we use the Green's function method to give the general formulas of the linear and nonlinear magnetization. These formulas can be adopt to evaluate the spin susceptibilities for altermagnet/superconductor heterostructures. In this subsection, we provide the analytical solution of the nonlinear spin susceptibility χ_{ab}^z . For the altermagnets, we can write down a general two-band model

$$H_{\mathbf{k}} = [t a^2 (k_x^2 + k_y^2) - \mu] s_0 + J_{ex} a^2 [2k_x k_y \cos(2\theta) + (k_x^2 - k_y^2) \sin(2\theta)] s_z \quad (\text{S13})$$

t parameterizes the usual kinetic energy, J_{ex} denotes the d -wave exchange magnetic order parameter and μ is the chemical potential. θ is the angle between the altermagnetic orientation and the crystalline axes. The velocity operators are

$$\hat{v}_x = a^2 \begin{pmatrix} 2tk_x s_0 + 2J_{ex} k \sin(\phi + 2\theta) s_z & 0 \\ 0 & 2tk_x s_0 + 2J_{ex} k \sin(\phi + 2\theta) s_z \end{pmatrix}, \quad (\text{S14})$$

$$\hat{v}_y = a^2 \begin{pmatrix} 2tk_y s_0 + 2J_{ex} k \cos(\phi + 2\theta) s_z & 0 \\ 0 & 2tk_y s_0 + 2J_{ex} k \cos(\phi + 2\theta) s_z \end{pmatrix}, \quad (\text{S15})$$

and

$$\hat{w}_{xx} = a^2 \begin{pmatrix} 2ts_0 + 2J_{ex} \sin(2\theta) s_z & 0 \\ 0 & -2ts_0 - 2J_{ex} \sin(2\theta) s_z \end{pmatrix}, \hat{w}_{xy} = a^2 \begin{pmatrix} 2J_{ex} \cos(2\theta) s_z & 0 \\ 0 & -2J_{ex} \cos(2\theta) s_z \end{pmatrix}, \quad (\text{S16})$$

Here $k_x = k \cos(\phi)$ and $k_y = k \sin(\phi)$. For $J_{ex} \ll t$, we can obtain an approximate analytical results (using *Mathematica*) as $\chi_{xx}^z = \mu_B \sin(2\theta) \int_0^\infty f(x) dx + \mathcal{O}(J_{ex}^2)$ and $\chi_{xy}^z = \chi_{yx}^z = \mu_B \cos(2\theta) \int_0^\infty f(x) dx + \mathcal{O}(J_{ex}^2)$, where

$$f(x) = \frac{\beta^3 J_{ex}}{64\pi} x \operatorname{sech}^2 \gamma \left[\frac{4}{\beta^2} + t^2 x^4 (2 - 3 \operatorname{sech}^2 \gamma) + \frac{4tx^2(\mu - tx^2) \tanh \gamma}{\gamma} \right], \quad (\text{S17})$$

where $\gamma = \beta \sqrt{\Delta^2 + (tx^2 - \mu)^2} / 2$.

II. PAIRING CORRELATIONS

Although we only consider the simplest conventional spin singlet pairing, i.e., $\Delta_0 i s_y$, here we show that the d -wave magnetic order will induce the spin-triplet correlations. To show this, the BdG Hamiltonian is

$$\mathcal{H}_{\text{BdG}}^{\mathbf{k}} = \begin{pmatrix} H_{\mathbf{k}} & \Delta_0 i s_y \\ (\Delta_0 i s_y)^\dagger & -H_{-\mathbf{k}}^* \end{pmatrix} \quad (\text{S18})$$

Here $H_{\mathbf{k}}$ is from Eq.(S13). Let us identify the superconducting properties in terms of Green's function:

$$G_{\lambda\mu}(\mathbf{k}, \tau) = T_\tau \{ c_{\mathbf{k},\lambda}(\tau) c_{\mathbf{k},\mu}^\dagger(0) \}, \quad (\text{S19})$$

$$F_{\lambda\mu}(\mathbf{k}, \tau) = T_\tau \{ c_{\mathbf{k},\lambda}(\tau) c_{-\mathbf{k},\mu}(0) \}. \quad (\text{S20})$$

We can rewrite the Green's function in the Matsubara frequency space: $G_{\lambda\mu}(\mathbf{k}, i\omega_n) = \int_0^\beta d\tau e^{i\omega_n \tau} G_{\lambda\mu}(\mathbf{k}, \tau)$ and $F_{\lambda\mu}(\mathbf{k}, i\omega_n) = \int_0^\beta d\tau e^{i\omega_n \tau} F_{\lambda\mu}(\mathbf{k}, \tau)$. The latter $F_{\lambda\mu}(\mathbf{k}, i\omega_n)$ represents the pairing correlations we refer. These two Green's functions are related to the Gor'kov Green's function as

$$\mathcal{G}(\mathbf{k}, i\omega_n) = (i\omega_n - H_{\text{BdG}}^{\mathbf{k}})^{-1} = \begin{pmatrix} G_e(\mathbf{k}, i\omega_n) & F(\mathbf{k}, i\omega_n) \\ F^\dagger(\mathbf{k}, i\omega_n) & G_h(\mathbf{k}, i\omega_n) \end{pmatrix}. \quad (\text{S21})$$

Substitute the BdG Hamiltonian into Eq. (S21) and after some massage, we can parameterize the pairing correlation as

$$F(\mathbf{k}, i\omega_n) = \Delta_0 [C_1(\mathbf{k}, i\omega_n) + C_2(\mathbf{k}, i\omega_n) \mathbf{d}(\mathbf{k}) \cdot \mathbf{s}] i s_y \quad (\text{S22})$$

with the coefficients

$$C_1(\mathbf{k}, i\omega_n) = -\frac{1}{2} \left[\frac{1}{\Delta_0^2 + \xi_k^2 - (J_{ex} f_k^2 + i\omega_n)^2} + \frac{1}{\Delta_0^2 + \xi_k^2 - (J_{ex} f_k^2 - i\omega_n)^2} \right], \quad (\text{S23})$$

$$C_2(\mathbf{k}, i\omega_n) = \frac{2i\omega_n}{(\Delta_0^2 + \xi_k^2 - J_{ex}^2 f_k^2)^2 + 2(\Delta_0^2 + \xi_k^2 + J_{ex}^2 f_k^2) \omega_n^2 + \omega_n^4}, \quad (\text{S24})$$

where $\xi_k = ta^2(k_x^2 + k_y^2) - \mu$ and $f_k = a^2[2k_x k_y \cos(2\theta) + (k_x^2 - k_y^2) \sin(2\theta)]$. Importantly, the triplet vector is directly related to the d -wave magnetic order with

$$\mathbf{d}(\mathbf{k}) = (0, 0, J_{ex} f_k), \quad (\text{S25})$$

Therefore, it can be seen that due to the presence of d -wave, the spin-singlet pairing and the spin-triplet pairing are mixed. Microscopically, the spin-singlet pairing correlations provide the physical origin of the nonlinear spin magnetization.

III. LINEAR EDELSTEIN EFFECT IN RASHBA-TYPE SUPERCONDUCTORS

In this section we review the linear magnetoelectric effect in superconductors with Rashba SOC. The low energy Bloch Hamiltonian is

$$H_{\mathbf{k}} = [ta^2(k_x^2 + k_y^2) - \mu] s_0 + \lambda a(k_x s_y - k_y s_x), \quad (\text{S26})$$

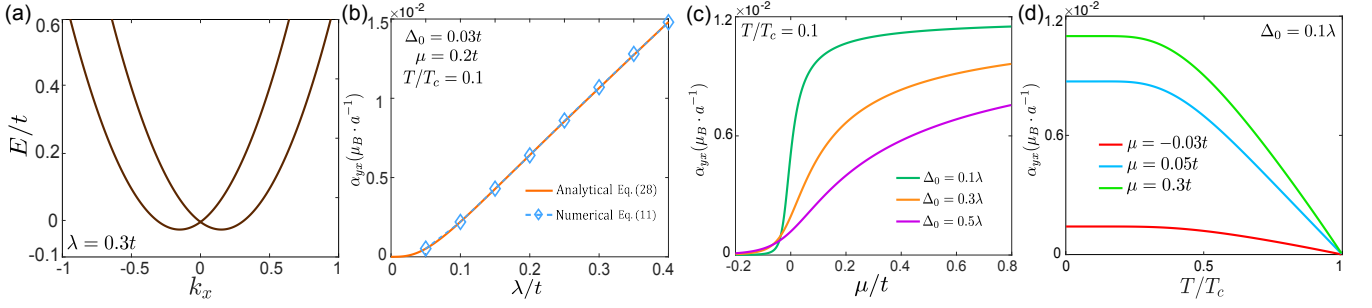


FIG. S1. The linear spin magnetization in Rashba-type superconductors. (a) The band structure with Rashba SOC at $\lambda = 0.3t$. (b) The first-order spin susceptibility α_{yx} as a function of λ at $T = 0.1T_c$, $\Delta_0 = 0.03t$ and $\mu = 0.2t$. The purple diamonds denotes the numerical results from Eq. (S11) and the orange line denotes the analytical result from Eq. (S28). (c) The first-order spin susceptibility α_{yx} as a function of μ at $T = 0.1T_c$ for various values of the pairing gap Δ_0 . (d) α_{yx} as a function of T at $\Delta_0 = 0.1\lambda$ for various values of μ .

where λ characterizes the strength of Rashba SOI, and a is the lattice constant. We introduce the spin singlet pairing $\Delta_{\mathbf{k}} = \Delta_0 i s_y$. Similarly, the linear spin susceptibility α_{yx} can be obtained as

$$\alpha_{yx} = \mu_B \int_0^\infty f(x) dx \quad (\text{S27})$$

where

$$f(x) = \frac{\beta}{32\pi(tx^2 - \mu)} \{x(\lambda - 2tx)(tx^2 - \mu)\text{sech}^2\gamma_1 + x(\lambda + 2tx)(tx^2 - \mu)\text{sech}^2\gamma_2 - [\Delta^2 + (\mu - tx^2)(\mu + \lambda x - tx^2)] \tanh \gamma_1/\gamma_1 + [\Delta^2 + (\mu - tx^2)(\mu - \lambda x - tx^2)] \tanh \gamma_2/\gamma_2\} \quad (\text{S28})$$

with

$$\gamma_1 = \frac{\beta \sqrt{\Delta^2 + (\mu + \lambda x - tx^2)^2}}{2}, \gamma_2 = \frac{\beta \sqrt{\Delta^2 + (\mu - \lambda x - tx^2)^2}}{2} \quad (\text{S29})$$

We apply the above formula to calculate the linear (first order) magnetization in superconductors with Rashba SOI. The calculated band structure from Eq. (S26) is shown in Fig. S1(a) at $\lambda = 0.3t$. By employing Eq. (S28), we plot the α_{yx} as a function of λ in Fig. S1 (orange solid curve). By way of comparison, we also show a fully numerical plot of Eq. (S11) (blue diamonds); both agree with each other. In Fig. S1(c) we show the μ -dependence of the α_{yx} with various values of Δ_0 . When $\mu < 0$, α_{yx} decreases as μ goes down. Fig. S1(d) shows α_{yx} as a function of temperature for different values of μ . Generally, α_{yx} starts to grow linearly when $T < T_c$, and it saturates when $T \rightarrow 0$. These behaviors are consistent with the results shown in Ref. [13].